

Research Paper

Probing Beta Relaxation in Pharmaceutically Relevant Glasses by Using DSC

Sergey Vyazovkin^{1,2} and Ion Dranca¹

Received July 25, 2005; accepted October 6, 2005

Purpose. This study was conducted to demonstrate the use of differential scanning calorimetry (DSC) in detecting and measuring β -relaxation processes in amorphous pharmaceutical systems.

Methods. DSC was employed to study amorphous samples of poly(vinylpyrrolidone) (PVP), indomethacin (IM), and ursodeoxycholic acid (UDA) that were annealed at temperatures (T_a) around 0.8 of their glass transition temperatures (T_g). Dynamic mechanical analysis (DMA) was used to measure β -relaxation in PVP.

Results. Reheating the annealed samples gives rise to annealing peaks that occur below T_g . The peaks cannot be generated when annealing below the low temperature limit of β -relaxation. These limits are around 50°C for PVP, -20°C for IM, and 30°C for UDA. The effective activation energy (E) of the sub- T_g relaxation has been estimated for each T_a and found to increase with T_a , reflecting increasing contribution of the α -process. Estimates of E for β -relaxation have been obtained from the lowest T_a data, and are as follows: 68 (PVP), 56 (IM), 67 (UDA) kJ mol⁻¹.

Conclusions. DSC can be used for detecting β -relaxation processes and estimating its low temperature limit, i.e., the temperature below which amorphous drugs would remain stable. It can also provide comparative estimates of low temperature stability of amorphous drugs in terms of the activation energies of the β -relaxation.

KEY WORDS: amorphous systems; differential scanning calorimetry (DSC); kinetics; molecular mobility.

INTRODUCTION

Although glassy amorphous pharmaceuticals feature enhanced bioavailability, they are thermodynamically unstable and tend to relax toward the stable crystalline state. The relaxation dynamics slows down dramatically when glasses are cooled below their glass transition temperature (T_g). It is generally believed that about 50°C below T_g the relaxation rate becomes so slow that glassy pharmaceuticals may be considered stable for all practical purposes. This conclusion is typically arrived at by measuring the relaxation times of α -relaxation (i.e., the glass transition) and extrapolating them to lower temperatures. However, this approach does not account for β -relaxation that is associated with the local noncooperative molecular motion. Compared to the cooperative α -processes, the β -processes have a significantly lower activation energy. For this reason, the β -process persists at markedly lower temperatures and becomes the major relaxation mechanism for aging glassy materials well below their T_g (1). Comparative dynamics of the α - and β -processes is presented schematically in Fig. 1. It should be noted that in the glassy state these processes couple, giving rise to a broad spectrum of the overall relaxation times. The faster part of

the spectrum is related to the β -process, whereas the slower part is associated with the α -process. Separation of the processes is typically accomplished via mechanical and/or dielectric spectroscopy (2,3) that allows one to vary frequency and, therefore, to detect the processes whose relaxation time matches the frequency of the probe.

Without varying the frequency, the separation can be accomplished at least partially by annealing (aging) a glassy material well below T_g . Under these conditions, annealing unfreezes the faster part of the overall relaxation spectrum, i.e., the part associated predominantly with the β -process. The lower the temperature and annealing time, the larger the contribution of the β -process to the overall relaxation. This property allows techniques such as differential scanning calorimetry (DSC) to be used for probing β -relaxations. When a glass is annealed well below its T_g , it slowly relaxes and loses its enthalpy. By reheating the annealed glass after quick cooling, the lost enthalpy is recovered and can be detected in DSC as a small endothermic peak that precedes the glass transition step. By increasing the time of annealing, the peak increases in size, shifts to higher temperatures, overlapping with the glass transition, and, ultimately, emerging as a large enthalpy overshoot at the end of the glass transition (4-6). The effect was extensively studied by Chen (4) for metallic and inorganic glasses, and by Bershtein and Egorov (5) for polymers. The latter authors (5) linked the β -process to the annealing peaks by demonstrating for a number of polymers that the peaks arise on annealing in the

¹ Department of Chemistry, University of Alabama at Birmingham, 901 S. 14th Street, Birmingham, Alabama 35294, USA.

² To whom correspondence should be addressed. (e-mail: vyazovkin@uab.edu)

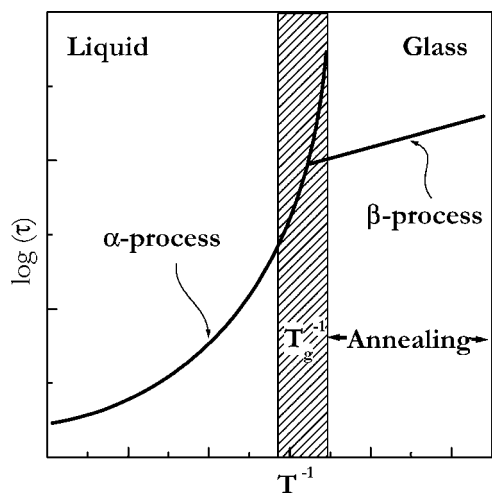


Fig. 1. Temperature dependence of relaxation times for the α - and β -processes. Hatched area represents the region around T_g , where the α - and β -processes are strongly coupled.

temperature region of β -relaxation, and that the activation energy, E , evaluated from the shift of the peak temperature, T_p , with the heating rate, q , as

$$E = -R \frac{d \ln q}{dT_p^{-1}} \quad (1)$$

has values similar to those obtained from dielectric and mechanical spectroscopy. The aforementioned book (5) provides a detailed discussion of using DSC for measuring and understanding the β -relaxations. Equation (1) was also widely used by Chen, who found in his study of metallic and inorganic glasses that the resulting E values are significantly smaller than the activation energies of α -relaxation.

Alternatively, Hodge and Berens (7) showed that the annealing peaks can be simulated in the framework of the Tool (8)–Narayanaswamy (9)–Moynihan (10,11) (TNM) model by substituting in it the activation energy of the α -relaxation and varying other parameters of the model. However, this cannot be taken as a proof that the activation energy of the process behind the annealing peak is similar to that of the α -relaxation. First, in addition to a number of known shortcomings (12), the TNM model is generally not capable of describing annealing at temperatures significantly below T_g (13,14), and the region of its quantitative application does not extend further than $\sim 20^\circ\text{C}$ below T_g (15). On the other hand, the model has four parameters that gives it ample fitting flexibility regardless of a physical meaning of the fit. Second, there is substantial experimental evidence that the annealing process at temperatures far below T_g demonstrates the activation energy that is several times smaller than that of the α -process (16).

In this paper, we demonstrate that β -relaxations in pharmaceutical glasses can be probed via DSC measurements of the aforementioned annealing effects. We apply this method to several pharmaceutically relevant glasses that include poly(vinylpyrrolidone) (PVP), indomethacin (IM), and ursodeoxycholic acid (UDA) and demonstrate that the E values obtained by Eq. (1) are consistent with the activation energies of the β -relaxation. The consistency is confirmed by comparing the obtained E values with independent measure-

ments, literature values, and the empirical correlation, $E_\beta = (24 \pm 3)RT_g$, discovered by Kudlik *et al.* (17) and confirmed by other workers (18). The current literature on β -relaxations in pharmaceutical glasses is scarce at best, although some important studies have recently began by using the method of thermally stimulated depolarization current (TSDC) (19–21). Yet, the importance of the low temperature mobility for physical stability of amorphous pharmaceuticals is well recognized (22,23). We hope that the present study will expand a set of tools for probing β -relaxations in pharmaceutical systems and initiate further work in that important area.

EXPERIMENTAL

PVP (MW $\sim 8,000$) was purchased from Fisher. Indomethacin and ursodeoxycholic acid were purchased from MP Biomedicals, LLC. All the substances were used without further purification. For the annealing (β -relaxation) measurements, about 20 mg of crystalline IM or UDA was placed in 40- μL Al pans and heated to $\sim 15^\circ\text{C}$ above their respective melting points, 160 and 205°C . In the case of PVP, the samples were about 12 mg and heating was conducted up to $\sim 70^\circ\text{C}$ above its glass transition temperature of 140°C . Immediately after heating, the samples were quenched into liquid nitrogen and quickly placed into the DSC (Mettler-Toledo DSC 822 $^\circ$) that was maintained at 20°C for PVP and UDA and at -40°C for IM runs. After a short period of stabilization at the initial temperature, the samples were heated to an annealing temperature, T_a , and maintained for 30 min. The annealing temperatures were -20 , -10 , and 0°C for IM; 50, 60, 70, 80, and 90°C for PVP; and for 30, 40, 50, and 60°C for UDA. After completion of the annealing segment, the samples were cooled down either to -10°C (PVP and UDA) or to -40°C (IM), and immediately heated above T_g . The heating rates were 10, 15, 20, 25, and $30^\circ\text{C min}^{-1}$. The resulting endothermic peaks observed on heating were used to determine the peak temperature, T_p , by using the standard DSC software that subtracts extrapolated baseline and finds the peak position.

Dynamic mechanical analysis (DMA) measurements were performed on PVP films cast from a methanol solution into a Petri dish. The solvent was then vaporized under the hood at room temperature. The resulting film was ~ 0.3 mm thick. The film was cut to rectangular pieces of $\sim 11 \times 7$ mm. Based on thermogravimetry (Mettler-Toledo TGA/SDTA851 $^\circ$), the films contained around $\sim 15\%$ of the solvent that was lost by 100°C . To remove the solvent, the films were dried for about 10 min at 110°C immediately before DMA runs. These films contained only about 1% of the residual solvent and/or moisture. The dried films were clumped in the tension frame of a Tritec 2000 DMA (Triton Technology Ltd.) and heated from room temperature to the glass transition region at a heating rate 2°C min^{-1} and a strain amplitude 0.05 mm. The runs were carried out at frequencies 0.3, 1, 3, and 10 Hz.

RESULTS AND DISCUSSION

Poly(vinylpyrrolidone)

Early dielectric spectroscopy measurements (24) on PVP were performed markedly below its T_g value and showed

only one peak in $\tan \delta$ around -70°C at 1 kHz that was assigned to β -relaxation. More recent dielectric measurements (25) were performed at 20 Hz–20 kHz, and demonstrated a strong dependence of relaxation peaks on the water content. Also, the data showed three $\tan \delta$ events that in PVP containing 23% w/w of water occurred at -100 to -80°C (assigned to β -relaxation based on previous work (24)), at $\sim 40^\circ\text{C}$ (assigned α -relaxation), and a shoulder preceding the α -relaxation that was not discussed. Most recently, Karabanova *et al.* (26) carried out DMA and dielectric spectroscopy (27) measurements on PVP and observed three $\tan \delta$ peaks in both types of measurements. In DMA (3–20 Hz), the peaks were found at $\sim -90^\circ\text{C}$ (assigned to β -relaxation), between 140 and 180°C (assigned to the glass transition), and between 50 and 70°C . The later peak was assigned to the second glass transition, although this effect was “not obvious from the DSC measurement” (26). Dielectric measurements (1–20 kHz) demonstrated three $\tan \delta$ peaks at -100 to 0, 50 to 100, 125 to 175°C , which were also interpreted as β -relaxation and two glass transitions, respectively.

Our measurements were performed from 25°C to the initial stages of the glass transition that occurs just above $T_g \sim 140^\circ\text{C}$ detected by DSC measurements. The glass transition (i.e., α -relaxation) is preceded by a lower temperature $\tan \delta$ peak that occurs around 50°C at the lowest frequency and around 100°C at the highest frequency (Fig. 2). Our DSC measurements did not show any thermal events in that temperature region. The $\tan \delta$ peaks preceding the α -relaxation are commonly (3) assigned to β -relaxation that typically occurs around $0.75T_g$ (28) (reportedly (5) actual values may span from 0.65 to $0.85T_g$). In a view of this correlation, if the aforementioned assignments of β -relaxation are correct, the glass transition should be observed well below 0°C , which is clearly not the case. On the other hand, based on the DSC measured value of T_g , β -relaxation should be expected to occur around 50°C . This corresponds fairly well to the temperature region of the effect observed in our measurements as well as to the temperature region of the “second glass transition” observed in DMA and dielectric measurements by other groups (26,27). Note that recent TSDC measurements (21) on PVP (MW $\sim 50,000$) also showed a smaller peak around 120 – 130°C (interpreted as β -relaxation) followed by the major α -relaxation event at 170 – 180°C .

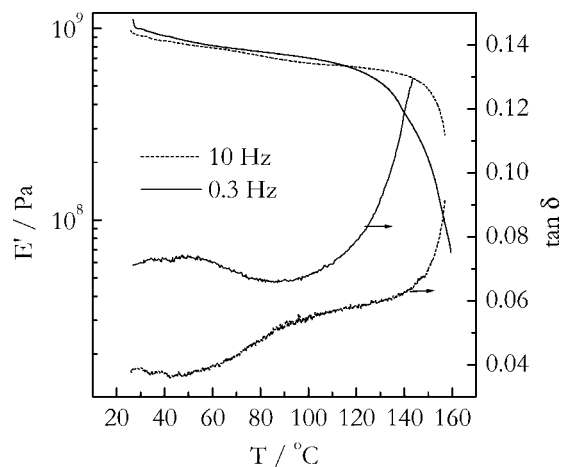


Fig. 2. DMA data (storage modulus, E' , and loss tangent, $\tan \delta$) for PVP sample at the two extreme frequencies.

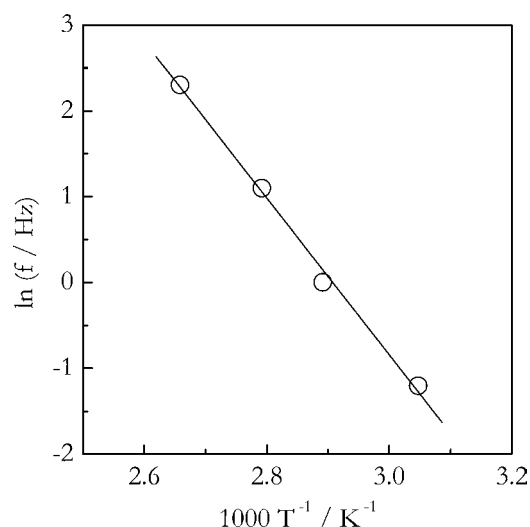


Fig. 3. Arrhenius plot for the frequency dependency of the peak temperature.

By using the shift in the peak temperature, T_p as a function of frequency, f , we evaluated the activation energy of the respective relaxation process as

$$E = -R \frac{d \ln f}{dT_p^{-1}} \quad (2)$$

Figure 3 displays the respective Arrhenius plot that yields $E = 76 \pm 10 \text{ kJ mol}^{-1}$. This value fits well in the aforementioned correlation $E_\beta = (24 \pm 3)RT_g$ (Fig. 4). On the other hand, the process observed by dielectric spectroscopy around -70°C and interpreted as β -relaxation yielded activation energy $\sim 46 \text{ kJ mol}^{-1}$ (24). Subject to the above correlation, this value gives rise to the glass transition temperature well below 0°C that disagrees with the experiment. Therefore, we believe that the lower temperature relaxation should rather be interpreted as γ -relaxation, whereas the peak occurring in

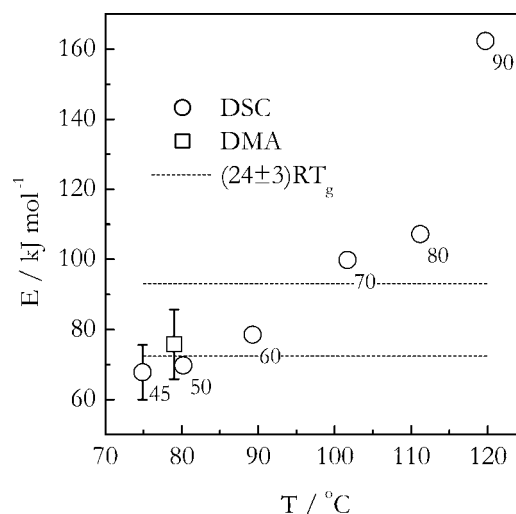


Fig. 4. Variation of the effective activation energy with the average peak temperature for DSC and DMA data on PVP. Numbers by the points represent annealing temperatures. Error bars are confidence intervals. Dash lines set lower and upper limits for $(24 \pm 3)RT_g$.

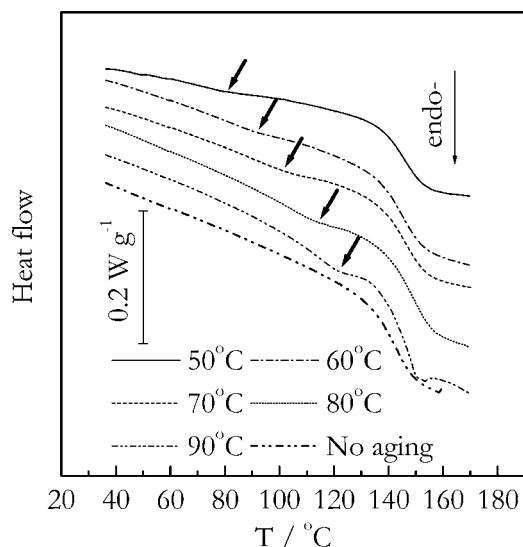


Fig. 5. DSC curves obtained on heating of PVP at $20^\circ\text{C min}^{-1}$ after annealing for 30 min at different T_a . “No aging” denotes a curve produced without annealing. Arrows show the location of the annealing effect.

the higher temperature region preceding the glass transition should be assigned to β -relaxation.

The annealing peaks can be easily obtained when a glass is annealed in the temperature region of β -relaxation. A typical region of annealing temperatures starts around $0.8T_g$. Annealing of a glass in this temperature region causes an appreciable loss of the enthalpy. Cooling down and reheating of the annealed glass allows the lost enthalpy to be recovered that is typically detected in DSC as a broad and shallow endothermic effect (“annealing peak”), which starts to evolve just above the annealing temperature. Although broad and shallow, the peaks can be readily noticed when comparing a DSC curve for an annealed sample with that for a sample that is not aged, which demonstrates a practically straight baseline before the glass transition step (cf., Fig. 5).

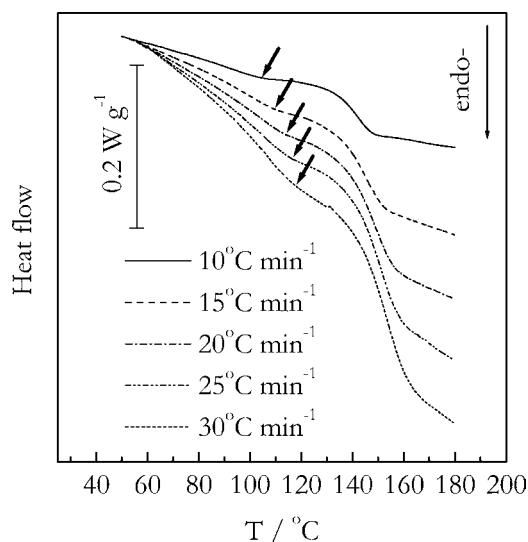


Fig. 6. DSC curves obtained on heating of PVP at different heating rates after annealing for 30 min at 80°C . Arrows show the location of the annealing effect.

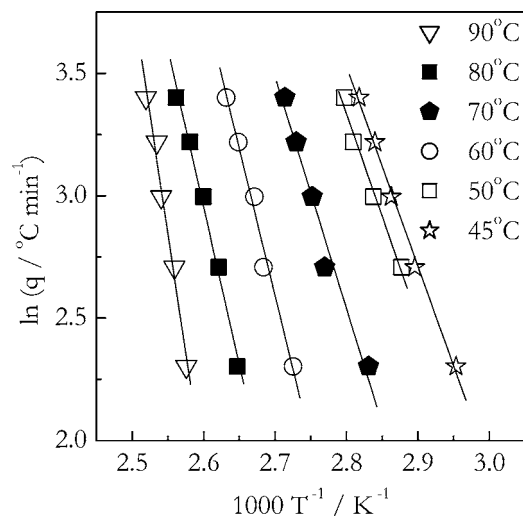


Fig. 7. Evaluating effective activation energies from annealing peaks of PVP annealed at different temperatures (shown by respective symbols).

Figure 5 presents a series of annealing peaks obtained on PVP samples annealed at different T_a and reheated at $20^\circ\text{C min}^{-1}$. It is seen that at the lowest $T_a = 50^\circ\text{C}$ the peak is completely separated from the glass transition step, whereas at the highest $T_a = 90^\circ\text{C}$, the higher temperature wing of the peak overlaps with the glass transition. For each annealing temperature, the annealed samples were reheated at different heating rates that allowed us to produce a shift in the peak temperature, and, thus to evaluate the effective activation energy by Eq. (1). An example of such a shift is shown in Fig. 6. The respective Arrhenius plots are shown in Fig. 7. It is seen that the plots are linear as expected for β -relaxation (1–3). It is also seen that the slope of the plots increases with T_a that represents an increase in the effective activation energy with increasing the average temperature of the annealing peak (Fig. 4). The average temperature was evaluated as the mean value of the peak temperatures detected at different heating rates. The increase reflects the aforementioned coupling of the β - and α -processes (Fig. 1). Annealing at the lower temperatures mostly unfreezes the faster part of the overall relaxation times distribution, which is the part that represents the local molecular motion of individual molecules or individual segments of a polymer chain. This type of motion is customarily identified with the β -process. At higher temperatures, the local motion intensifies, initiating the cooperative motion of nearby molecules or segments. The cooperative motion is recognized as the α -process representing the slower part of the overall relaxation times distribution. The activation energy of the α -process is typically several times larger than that of the β -process. Therefore, increase in E with T_a (Fig. 4) reflects an increasing contribution of the cooperative α -motion to the annealing process. In other words, annealing at the lowest feasible temperature should yield the most accurate estimate for the activation energy of the β -process. The E value related to $T_a = 50^\circ\text{C}$ is 69.7 kJ mol^{-1} . No reliable detection of annealing peaks was possible at $T_a = 40^\circ\text{C}$. Evaluating this temperature limit can be critical in estimating the physical stability of glassy pharmaceuticals, because aging is known (29) to practically stop below the temperature

region of β -relaxation. However, we were able to measure the effect at $T_a = 45^\circ\text{C}$ that gave rise to the E value $68 \pm 8 \text{ kJ mol}^{-1}$, which we consider to be an estimate of the effective activation energy for β -relaxation in PVP. As shown in Fig. 4, this value agrees well with the correlation, $E_\beta = (24 \pm 3)RT_g$ (T_g measured by DSC is $\sim 140^\circ\text{C}$) as well as with the value derived from DMA data. We would also like to stress that the annealing peaks were observed when PVP was annealed in the temperature region of β -relaxation as measured by DMA.

It should be noted that in their TSDC study, Shmeis *et al.* (21) also observed that the effective activation energy of the β -relaxation increases with the increase in polarization temperature. The effect is similar to that described in above (Fig. 4), and the lowest value of E accomplished in their runs is $\sim 63 \text{ kJ mol}^{-1}$, which is consistent with our estimate for the β -relaxation in PVP.

Indomethacin

The present data were collected as a part of a project aimed at demonstrating that crystallization of amorphous IM can occur in the temperature region of the β -relaxation (6). First, we conducted a set of trial 30-min annealing runs at T_a from -30 to 20°C in incremental steps of 10°C . However, the peaks were detected only for $T_a = -20, -10,$ and 0°C (Fig. 8). This was unexpected from the standpoint of our previous experience with polystyrene systems (30) and our present work with PVP, for which the peaks are reliably detectable for the interval of T_a that covers more than 40°C . To look closer into this problem, we performed a few 3-h annealing runs at $T_a = -30, 10,$ and 20°C . No peaks were produced after annealing at -30°C that suggests this temperature could be an estimate of the lower temperature limit for β -relaxation. On annealing at 10°C , the effect was found to strongly overlap with the glass transition step that prevented us from detecting it at annealing for 30 min. Annealing at

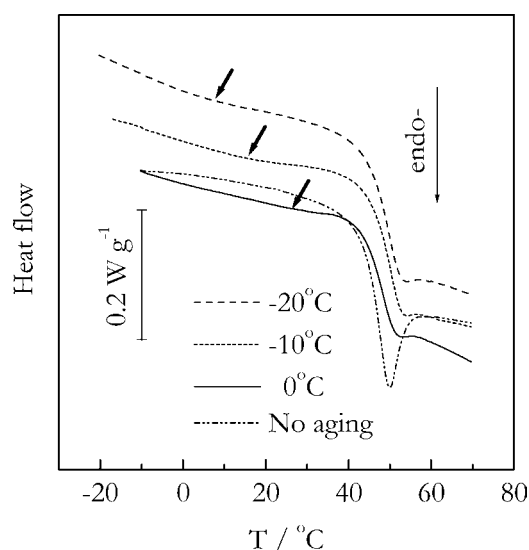


Fig. 8. DSC curves obtained on heating of IM at $20^\circ\text{C min}^{-1}$ after annealing for 30 min at different T_a . “No aging” denotes a curve produced without annealing. Arrows show the location of the annealing effect.

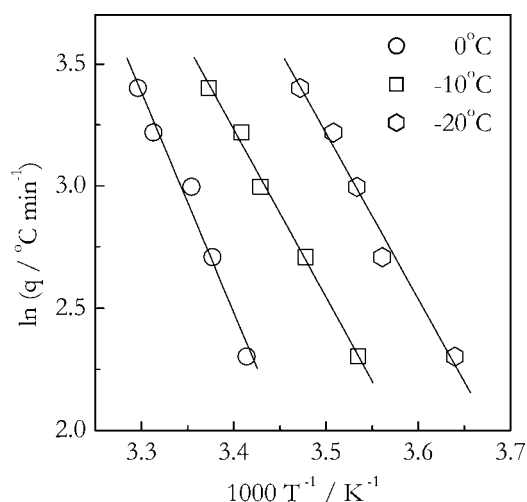


Fig. 9. Evaluating effective activation energies from annealing peaks of IM annealed at different temperatures (shown by respective symbols).

20°C resulted in obtaining of a larger enthalpy overshoot as it is typically discovered in glasses aged not far below T_g . The observed strong shift of the annealing peaks with T_a provides a clear indication that the respective relaxation process occurs with a low effective activation energy.

The E values were determined for the three annealing temperatures ($-20, -10,$ and 0°C) by using Eq. (1). The resulting $\ln q$ against T_p^{-1} plots are shown in Fig. 9. The plot for $T_a = 0^\circ\text{C}$ gives $E = 74.8 \text{ kJ mol}^{-1}$. For $T_a = -20$ and -10°C , the plots are almost parallel and yield practically equal values of the activation energy. A dependence of the effective activation energy of the annealing peak on its average temperature is displayed in Fig. 10. The E values show an increasing trend similar to that observed in PVP (Fig. 4). The E value related to the lowest $T_a = -20^\circ\text{C}$ is $56 \pm 12 \text{ kJ mol}^{-1}$ provides an estimate for the β -relaxation process. This value fits well into the correlation, $E_\beta = (24 \pm 3)RT_g$, when substituting $T_g = 46^\circ\text{C}$ as measured by DSC.

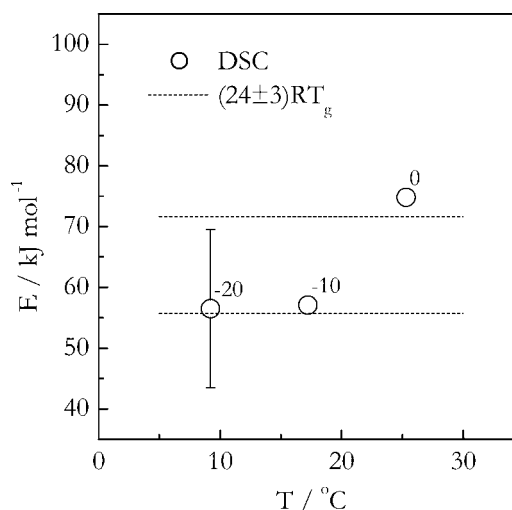


Fig. 10. Variation of the effective activation energy with the average peak temperature for DSC data on IM. Numbers by the points represent annealing temperatures. Error bars are confidence intervals. Dash lines set lower and upper limits for $(24 \pm 3)RT_g$.

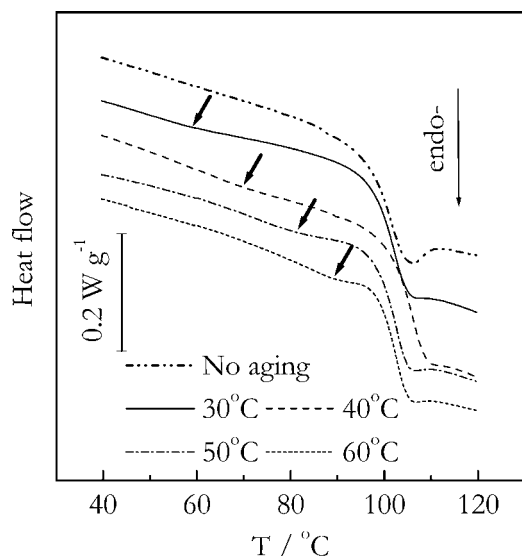


Fig. 11. DSC curves obtained on heating of UDA at $20^{\circ}\text{C min}^{-1}$ after annealing for 30 min at different T_a . “No aging” denotes a curve produced without annealing. Arrows show the location of the annealing effect.

The obtained results are in good agreement with the TSDC data by Correira *et al.* (19), who discovered three different temperature regions of mobility in glassy IM. The higher temperature region was attributable to regular glass transition (α -relaxation) that becomes detectable above 35°C . In addition, two secondary relaxation processes were observed in the respective temperature regions -160 to -80 and 0 to 30°C . Because the high temperature process is α -relaxation, the lower temperature process occurring at 0 – 30°C should be interpreted as β -relaxation. Note that this is practically the same region where we observed the appearance of the annealing peaks (Figs. 8 and 10). In evaluating the effective activation energy of the respective relaxation process, Correira *et al.* (19) also observed that E increases from 66 to 85 kJ mol^{-1} with increasing the polarization temperature. Assuming that the increase is a

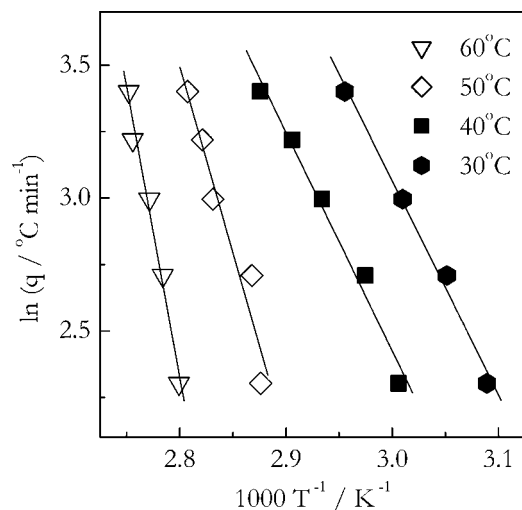


Fig. 12. Evaluating effective activation energies from annealing peaks of UDA annealed at different temperatures (shown by respective symbols).

result of the increasing contribution of the α -process, the E value obtained at the lowest polarization temperature (i.e., 66 kJ mol^{-1}) should provide the closest estimate for the activation energy of the β -relaxation in indomethacin. This estimate is obviously consistent with ours.

Ursodeoxycholic Acid

Although UDA has been thermally well characterized (31) and its glass transition kinetics have been examined (32), we are not aware of any reports on β -relaxation in this compound. Nevertheless, we chose UDA because it has the T_g value of around 100°C , which is intermediate between PVP and IM. Therefore, according to the aforementioned correlation, $E_{\beta} = (24 \pm 3)RT_g$, one can expect UDA to demonstrate an intermediate value of the activation energy for β -relaxation.

Figure 11 shows a shift of the annealing peaks with the annealing temperature. The value of T_a was changed in 10°C steps. We were not able to detect annealing peaks at $T_a = 20^{\circ}\text{C}$ that seems to be a limiting temperature for β -relaxation in UDA. Above 60°C , annealing peaks strongly overlapped with the glass transition step. Therefore, the experiments carried out $T_a = 30, 40, 50,$ and 60°C were used for evaluating the effective activation energy of the respective relaxation process. Plots of $\ln q$ against T_p^{-1} are presented in Fig. 12. The slope of the plot decreases with decreasing T_a as in the two previous cases (Figs. 7 and 9), suggesting a decrease in the effective value of E . Clearly, the resulting dependence of the activation energy on the average temperature of the annealing peak demonstrates (Fig. 13) a pattern similar to that for PVP and IM. Following the same physical reasoning, we can conclude that the E value $67 \pm 12 \text{ kJ mol}^{-1}$ obtained at the lowest $T_a = 30^{\circ}\text{C}$ provides an estimate for the activation energy of β -relaxation in UDA. As seen in Fig. 13, the obtained estimate is consistent with $E_{\beta} = (24 \pm 3)RT_g$. As expected from the T_g value, the activation energy for UDA is bigger than that for IM, although it is practically equal to the activation energy of PVP.

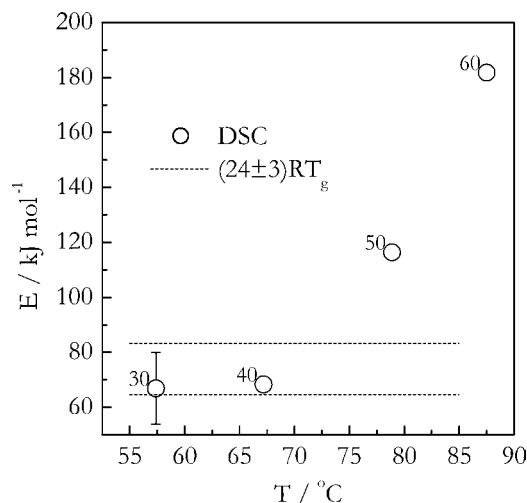


Fig. 13. Variation of the effective activation energy with the average peak temperature for DSC data on UDA. Numbers by the points represent annealing temperatures. Error bars are confidence intervals. Dash lines set lower and upper limits for $(24 \pm 3)RT_g$.

CONCLUSIONS

DSC has been employed for probing β -relaxations in pharmaceutical glasses annealed at temperatures around $0.8T_g$. The resulting annealing peaks have been used for estimating the low temperature limit of β -relaxation, i.e., the temperature below which amorphous drugs would remain practically stable. A shift in the peak temperature with the heating rate allows one to obtain a trustworthy estimate for the activation energy of β -relaxation. The trustworthiness of the estimates has been tested by comparing them against independent estimates obtained by DMA, TSDC as well as by relationship $E_\beta = (24 \pm 3)RT_g$. More than satisfactory agreement has been observed for all studied systems.

ACKNOWLEDGMENT

This work was partially supported by the Boehringer-Ingelheim Cares Foundation.

REFERENCES

1. E. Donth. *The Glass Transition: Relaxation Dynamics in Liquids and Disordered Materials*, Springer, Berlin, 2001.
2. P. Hedvig. *Dielectric Spectroscopy of Polymers*, Wiley, New York, 1977.
3. N. G. McCrum, B. E. Read, and G. Williams. *Anelastic and Dielectric Effects in Polymeric Solids*, Dover, New York, 1991.
4. H. S. Chen. On the mechanisms of structural relaxation in a $\text{Pd}_{48}\text{Ni}_{32}\text{P}_{20}$ glass. *J. Non-Cryst. Solids* **46**:289–305 (1981).
5. V. A. Bershtein and V. M. Egorov. *Differential Scanning Calorimetry of Polymers*, Ellis Horwood, New York, 1994.
6. S. Vyazovkin and I. Dranca. Physical stability and relaxation of amorphous indomethacin. *J. Phys. Chem., B* **109**:18637–18644 (2005).
7. I. M. Hodge and A. R. Berens. Effects of annealing and prior history on enthalpy relaxation in glassy polymers. 2. Mathematical modeling. *Macromolecules* **15**:762–770 (1982).
8. A. Q. Tool. Relation between inelastic deformability and thermal expansion in glass in its annealing range. *J. Am. Ceram. Soc.* **29**:240–253 (1946).
9. O. S. Narayanaswamy. A model of structural relaxation in glass. *J. Am. Ceram. Soc.* **54**:491–498 (1971).
10. C. T. Moynihan, A. J. Easteal, M. A. DeBolt, and J. Tucker. Dependence of the fictive temperature of glass on cooling rate. *J. Am. Ceram. Soc.* **59**:12–16 (1976).
11. M. A. DeBolt, A. J. Easteal, P. B. Macedo, and C. T. Moynihan. Analysis of structural relaxation in glass using rate heating data. *J. Am. Ceram. Soc.* **59**:16–21 (1976).
12. I. M. Hodge. Effects of annealing and prior history on enthalpy relaxation in glassy polymers. 6. Adam–Gibbs formulation of nonlinearity. *Macromolecules* **20**:2897–2908 (1987).
13. C. A. Angell, K. L. Ngai, G. B. McKenna, P. F. McMillan, and S. W. Martin. Relaxation in glassforming liquids and amorphous solids. *Appl. Phys. Rev.* **88**:3113–3157 (2000).
14. G. B. McKenna and S. L. Simon. In S. Z. D. Cheng (ed.), *Handbook of Thermal Analysis and Calorimetry*, vol. 3, Elsevier, Amsterdam, 2002, pp. 49–109.
15. J. M. Hutchinson. Physical aging of polymers. *Prog. Polym. Sci.* **20**:703–760 (1995).
16. S. V. Nemilov. Physical ageing of silicate glasses at room temperature: general regularities as a basis for the theory and the possibility of *a priori* calculation of the ageing rate. *Glass Phys. Chem.* **26**:511–530 (2000).
17. A. Kudlik, S. Benkhof, T. Blochowicz, C. Tschirwitz, and E. Rössler. The dielectric response of simple organic glass formers. *J. Mol. Struct.* **479**:201–218 (1999).
18. K. L. Ngai and S. Capaccioli. Relation between the activation energy of the Johari–Goldstein β relaxation and T_g of glass formers. *Phys. Rev., E* **69**:031501-1–031501-5 (2004).
19. N. T. Correia, J. J. M. Ramos, M. Descamps, and G. Collins. Molecular mobility and fragility in indomethacin: a thermally stimulated depolarization current study. *Pharm. Res.* **18**:1767–1774 (2001).
20. R. A. Shmeis, Z. Wang and S. K. Krill. A mechanistic investigation of an amorphous pharmaceutical and its solid dispersion. Part I. *Pharm. Res.* **21**:2025–2030 (2001).
21. R. A. Shmeis, Z. Wang, and S. K. Krill. A mechanistic investigation of an amorphous pharmaceutical and its solid dispersion. Part II. *Pharm. Res.* **21**:2031–2039 (2004).
22. B. C. Hancock, S. L. Shamblin, and G. Zografi. Molecular mobility of amorphous pharmaceutical solids below their glass transition temperatures. *Pharm. Res.* **12**:799–806 (1995).
23. S. L. Shamblin, X. Tang, L. Chang, B. C. Hancock, and M. J. Pikal. Characterization of the time scales of molecular motion in pharmaceutically important glasses. *J. Phys. Chem., B* **103**:4113–4121 (1999).
24. S. K. Jain and G. P. Johari. Dielectric studies of molecular motions in the glassy states of pure and aqueous poly(vinylpyrrolidone). *J. Phys. Chem.* **92**:5851–5854 (1988).
25. S. P. Duddu and T. D. Sokoloski. Dielectric analysis in the characterization of amorphous pharmaceutical solids. 1. Molecular mobility in poly(vinylpyrrolidone)—water systems in the glassy state. *J. Pharm. Sci.* **84**:773–776 (1995).
26. L. V. Karabanova, G. Boiteux, O. Gain, G. Seytre, L. M. Sergeeva, and E. D. Lutsyk. Semi-interpenetrating polymer networks based on polyurethane and polyvinylpyrrolidone. I. Thermodynamic state and dynamic mechanical analysis. *J. Appl. Polym. Sci.* **80**:852–862 (2001).
27. L. V. Karabanova, G. Boiteux, O. Gain, G. Seytre, L. M. Sergeeva, E. D. Lutsyk, and P. A. Bondarenko. Semi-interpenetrating polymer networks based on polyurethane and polyvinylpyrrolidone. II. Dielectric relaxation and thermal behaviour. *J. Appl. Polym. Sci.* **90**:1191–1201 (2003).
28. R. F. Boyer. Mechanical motions in amorphous and semi-crystalline polymers. *Polymer* **17**:996–1008 (1976).
29. L. C. E. Struik. *Physical Aging in Amorphous Polymers and Other Materials*, Elsevier, Amsterdam, 1978.
30. S. Vyazovkin and I. Dranca. A DSC study of α - and β -relaxations in a PS–clay system. *J. Phys. Chem., B* **108**:11981–11987 (2004).
31. E. Yonemochi, Y. Ueno, T. Ohmae, T. Oguchi, S. Nakajima, and K. Yamamoto. Evaluation of amorphous ursodeoxycholic acid by thermal methods. *Pharm. Res.* **14**:798–803 (1997).
32. K. J. Crowley and G. Zografi. The use of thermal methods for predicting glass-former fragility. *Thermochim. Acta* **380**:79–93 (2001).